

The W_t Transcendental Function and Quantum Mechanical Applications

V. E. Markushin ¹, R. Rosenfelder ¹ and A. W. Schreiber ²

¹ Paul Scherrer Institute, CH-5232 Villigen PSI, Switzerland

² Department of Physics and Mathematical Physics and Research Centre for the Subatomic Structure of Matter, University of Adelaide, Adelaide, S. A. 5005, Australia

Abstract

We discuss the function $W_t(x)$ defined via the implicit equation $W_t(x) \cdot \tan [W_t(x)] = x$, which appears in certain quantum mechanical and field theoretic applications. We investigate its analytic structure, develop series expansions for both small and large x , and provide various techniques for its numerical evaluation in the complex plane.

PACS-numbers: 02.30Gp, 02.30.Mv, 03.65.Db

1 Introduction

Implicit equations for functions appear frequently in physics although they are not discussed at all in standard handbooks on (standard) special functions [1, 2]. The most famous example, probably, is *Kepler's* equation

$$\omega t = \psi - e \sin \psi \tag{1.1}$$

which describes the dependence of the angle ψ (“the eccentric anomaly”) on the time t for an elliptical orbit with eccentricity e [3]. It has been a challenge to solve this equation for generations of astronomers and mathematicians, among them F. W. Bessel who was led by this problem to the functions which bear his name.

Another transcendental equation which has made its appearance in a variety of applications is

$$W(x) \exp [W(x)] = x , \tag{1.2}$$

the history of which goes back to J. H. Lambert and L. Euler in the 18th century. A comprehensive survey of the many available results for this function has been given in Ref. [4] where it has been called the *Lambert* W-function (probably because Euler already has enough named relations and functions to his credit ¹...). Apart from the examples given in the above article there is also some recent interest in the properties of $W(x)$ in particle [6] and nuclear physics [7].

Here we want to study a function defined by a superficially similar equation as given in (1.2), viz.

$$W_t(x) \cdot \tan [W_t(x)] = x \tag{1.3}$$

which, however, has a much richer structure than Lambert's W-function. Because of the similarity we propose to call ² the solution of Eq. (1.3) $W_t(x)$. Analogously, one could define

$$W_{ct}(x) \cdot \cot [W_{ct}(x)] = x \tag{1.4}$$

and $W_s(x)$ and $W_c(x)$. Eq. (1.3) emerged in a variational approach to Quantum Electrodynamics [8] where the relation between the bare mass and the physical mass of the electron was obtained in terms of the solution of an implicit equation of the type (1.3). However, as we will see in Section 2, the same equation also appears as an eigenvalue equation in a one-dimensional quantum mechanical problem for an infinite square well with a residual δ -function interaction. If the strength of this additional interaction is

¹In Ref. [5] a slightly more general equation is called “Ramanujan's equation”.

²“Names are important” [4] for a consistent nomenclature. In the present scheme the Lambert W-function would be denoted by $W_e(x)$.

constant one is naturally led to Eq. (1.4) whereas a linear energy dependence of this strength leads to Eq. (1.3).

In the present, mostly elementary, note we will concentrate on the W_t -function and, since we are not aware of any other systematic study, we will derive some representations by simple methods and study the interesting analytical structure of this function in the complex plane. We hope that this collection of results will be helpful for other applications where this function makes its appearance.

2 A quantum mechanical problem leading to $W_t(x)$

Consider a nonrelativistic particle moving in an one-dimensional infinite square well in $0 < \xi < a$. Assume that an attractive δ -function interaction is added in the middle of the interval whose strength is growing with the energy of the particle ³

$$\Delta V = -\lambda E \delta\left(\xi - \frac{a}{2}\right). \quad (2.1)$$

As the total Hamiltonian is symmetric with respect to transformations $\xi \rightarrow a - \xi$ the wave functions can be classified according to their symmetry under this transformation $\psi_n(\xi) = \pm\psi_n(a - \xi)$. Only the even wave functions are influenced by the additional interaction (2.1) since the odd wave functions vanish at $\xi = a/2$. The Schrödinger equation

$$-\frac{\hbar^2}{2m} \frac{d^2\psi(\xi)}{d\xi^2} - \lambda E \delta\left(\xi - \frac{a}{2}\right) \psi(\xi) = E\psi(\xi) \quad (2.2)$$

with $E = \hbar^2 k^2 / (2m)$ has the solutions

$$\psi(\xi) = \begin{cases} A_I \sin(k\xi) & , \quad 0 \leq \xi < a/2 \\ A_{II} \sin(k(a - \xi)) & , \quad a/2 < \xi \leq a. \end{cases} \quad (2.3)$$

The solution (2.3) fulfills the boundary conditions that the wave function has to vanish at the edges ($\xi = 0$ and $\xi = a$) of the infinite square well. At $\xi = a/2$ the wave function has to be continuous

$$A_I \sin\left(\frac{ka}{2}\right) = A_{II} \sin\left(\frac{ka}{2}\right), \quad (2.4)$$

but its derivative makes a jump proportional to the strength of the δ -function. This can be derived in the standard way by integrating Eq. (2.2) from $a/2 - \epsilon$ to $a/2 + \epsilon$ and letting $\epsilon \rightarrow 0$

$$-\frac{\hbar^2}{2m} \left[\frac{d\psi}{d\xi} \left(\frac{a}{2} + \epsilon\right) - \frac{d\psi}{d\xi} \left(\frac{a}{2} - \epsilon\right) \right] - \lambda E \psi\left(\frac{a}{2}\right) = 0. \quad (2.5)$$

³Energy-dependent potentials are frequently considered in nuclear and hadronic physics where they arise from eliminating part of the physical Hilbert space.

The r.h.s. vanishes since the wave function is finite and therefore its integral over an infinitesimal distance does not give a contribution. For our solutions this implies

$$A_{II} k \cos\left(\frac{ka}{2}\right) + A_I k \cos\left(\frac{ka}{2}\right) = \frac{2m}{\hbar^2} \lambda E A_I \sin\left(\frac{ka}{2}\right) = k^2 \lambda A_I \sin\left(\frac{ka}{2}\right). \quad (2.6)$$

Combining the boundary conditions (2.4) and (2.6) we obtain as eigenvalue condition ⁴

$$\frac{ka}{2} \tan\left(\frac{ka}{2}\right) = \frac{a}{\lambda} \quad (2.7)$$

with the general solution

$$k = \frac{2}{a} W_t\left(\frac{a}{\lambda}\right). \quad (2.8)$$

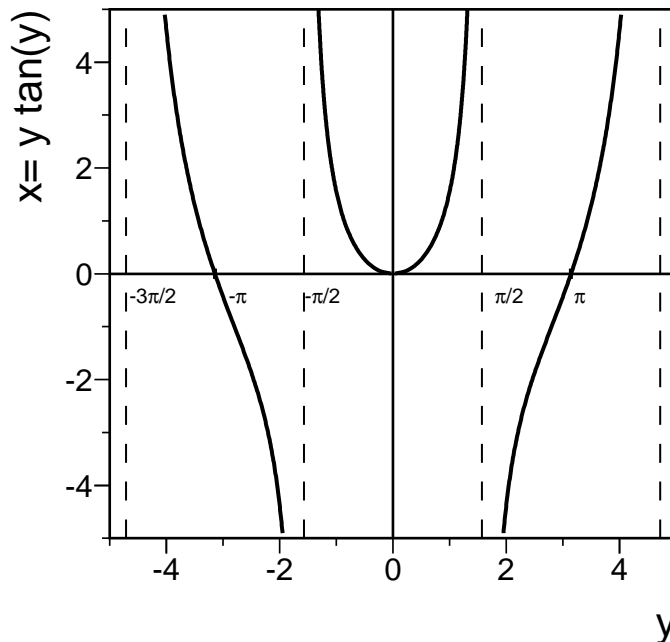


Figure 1: Eigenvalue equation (2.7) with $x = a/\lambda$ and $y = ka/2$.

The graphical representation of the eigenvalue equation in Fig. 1 shows that W_t is a *multivalued* function, and we have to define its branches. Our definition will be motivated by physical arguments: for vanishing interaction ($\lambda = 0$) the r.h.s. of Eq. (2.7) diverges and thus the tan-function has to diverge as well. Therefore

$$\frac{ka}{2} \Big|_{\lambda=0} = \pm \frac{\pi}{2}, \pm \frac{3\pi}{2}, \dots \quad (2.9)$$

⁴Note that the energy-dependence of the additional interaction is essential; without that one would obtain the relation $(ka/2) \cot(ka/2) = \lambda am/(2\hbar^2)$ leading to the W_{ct} -function.

which obviously gives the unperturbed wavenumbers (and hence energies) of the symmetric states in the infinitely deep square well of length a . Thus we define the n th branch of W_t by the requirement that $x = \infty$ is a regular point and

$$W_t^{(n)}(x \rightarrow \infty) = \text{sgn}(n) \left(|n| - \frac{1}{2} \right) \pi \quad , \quad n = \pm 1, \pm 2, \dots \quad (2.10)$$

The limit of very strong coupling ($\lambda \rightarrow \infty$) is also easily understood: if the δ -function is attractive the energy levels are lowered:

$$\frac{ka}{2} \Big|_{\lambda \rightarrow +\infty} = 0, \pm\pi, \dots \quad , \quad (2.11)$$

i.e.

$$W_t^{(n)}(x \rightarrow +0) = \text{sgn}(n) (|n| - 1) \pi \quad , \quad n = \pm 1, \pm 2, \dots \quad (2.12)$$

However, if the δ -function is very much repulsive the square well is practically halved and the eigenvalue condition is $\sin(ka/2) = 0$. This is formally the same as for $\lambda \rightarrow +\infty$ but $k = 0$ is excluded as trivial eigenvalue. Therefore the levels are pushed up:

$$\frac{ka}{2} \Big|_{\lambda \rightarrow -\infty} = \pm\pi, \pm 2\pi, \dots \quad (2.13)$$

i.e.

$$W_t^{(n)}(x \rightarrow -0) = n \pi \quad . \quad (2.14)$$

These conventions are summarized in Fig. 2. Since the value of $W_t(0)$ depends on the way one approaches the point $x = 0$, it must be a *branchpoint* for the function. Indeed, replacing for small argument the tan-function by its argument one finds for the principal branch (which corresponds to the ground state of the system)

$$W_t^{(1)}(x) \xrightarrow{x \rightarrow +0} \sqrt{x} \quad . \quad (2.15)$$

In general we have from eqs. (2.12, 2.14)

$$W_t^{(n)}(-0) = W_t^{(n+\text{sgn}(n))}(+0) \quad (2.16)$$

and our branch conventions can be summarized by writing the defining Eq. (1.3) in the form

$$W_t^{(n)}(x) = \text{sgn}(n) \left(|n| - \frac{1}{2} \right) \pi + \frac{1}{2i} \ln \left[\frac{x - iW_t^{(n)}(x)}{x + iW_t^{(n)}(x)} \right] \quad (2.17)$$

$$= \text{sgn}(n) \left(|n| - \frac{1}{2} \right) \pi + \Theta(-x) \text{sgn} [W_t^{(n)}(x)] \pi + \arg [x - iW_t^{(n)}(x)] \quad (2.18)$$

where $\ln(z)$ denotes the *principal* branch of the logarithmic function ($-\pi < \arg(z) \leq \pi$).

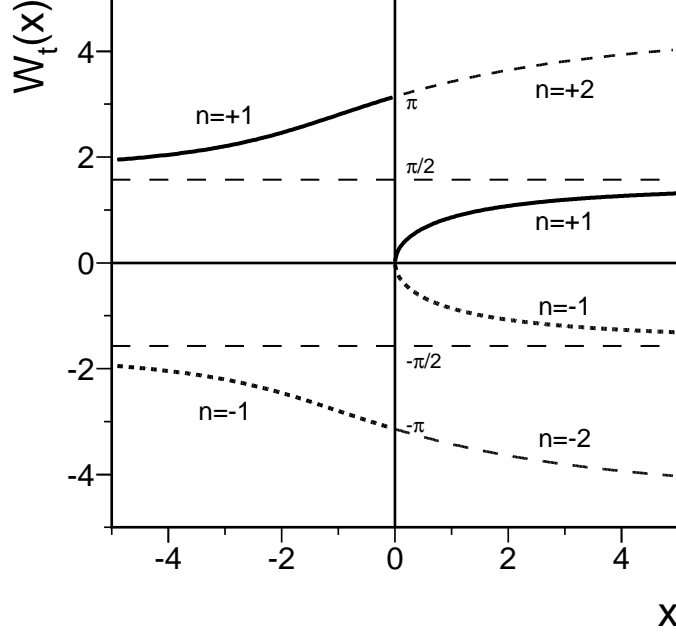


Figure 2: Branches of the W_t -function.

From Eq. (2.18) we obtain the important relation

$$\begin{aligned}
W_t^{(-n)}(x) &= -\text{sgn}(n) \left(|n| - \frac{1}{2} \right) \pi + \Theta(-x) \text{sgn} \left[W_t^{(-n)}(x) \right] \pi + \arg \left[x - iW_t^{(-n)}(x) \right] \\
&= -\text{sgn}(n) \left(|n| - \frac{1}{2} \right) \pi - \Theta(-x) \text{sgn} \left[-W_t^{(-n)}(x) \right] \pi - \arg \left[x + iW_t^{(-n)}(x) \right] \\
&= -W_t^{(n)}(x)
\end{aligned} \tag{2.19}$$

which allows us to restrict our analysis to branches with $n > 0$ (cf. Fig. 2). It is, of course, easy to find some special values of the W_t -function, e.g.

$$W_t^{(n+1)} \left(\frac{\pi}{4} + n\pi \right) = \frac{\pi}{4} + n\pi, \quad n = 0, 1, \dots \tag{2.20}$$

The above definition of the branches of $W_t^{(n)}(x)$ is still incomplete because we have not yet specified how different sheets of the Riemann surface are connected to each other across the cuts that must also be explicitly defined. This will be discussed in more detail in Section 5. In the next two Sections, our discussion concerns only the properties of the main branch $W_t^{(1)}(x)$ on the real x axis, where $W_t^{(1)}(x)$ is continuous except at the point $x = 0$.

3 Series expansions, differential equation and integrals

In this Section we concentrate on the the principal branch of the W_t -function, i.e. $n = 1$. From the defining equation (1.3) it is easy to obtain the first terms in the series expansion for small $x \geq 0$

$$W_t^{(1)}(x) = \sqrt{x} \sum_{k=0}^{\infty} a_k x^k = \sqrt{x} \left[1 - \frac{1}{6}x + \frac{11}{360}x^2 - \frac{17}{5040}x^3 - \frac{281}{604800}x^4 + \dots \right] \quad (3.1)$$

and, by setting $W_t = \pi(1 - v)/2$ for large $|x|$,

$$W_t^{(1)}(x) = \frac{\pi}{2} \sum_{k=0}^{\infty} \frac{b_k}{x^k} = \frac{\pi}{2} \left[1 - \frac{1}{x} + \frac{1}{x^2} - \left(1 - \frac{\pi^2}{12}\right) \frac{1}{x^3} - \left(\frac{\pi^2}{3} - 1\right) \frac{1}{x^4} + \dots \right]. \quad (3.2)$$

To calculate the expansion coefficients for $|x| \rightarrow \infty$ systematically, one may use Lagrange's expansion theorem for implicit functions ⁵:

$$b_0 = 1, \quad b_k = - \left(\frac{\pi}{2}\right)^k \frac{1}{k!} \frac{d^{k-1}}{dv^{k-1}} \left(\frac{v(1-v)}{\tan(\pi v/2)} \right)^k \Big|_{v=0}, \quad k \geq 1. \quad (3.3)$$

The convergence radii of the above two expansions may be estimated from the *root* test

$$x \leq \rho_0 = \lim_{k \rightarrow \infty} |a_k|^{-1/k} \equiv \lim_{k \rightarrow \infty} \rho_0^{(k)}, \quad |x| \geq \rho_\infty = \lim_{k \rightarrow \infty} |b_k|^{1/k} \equiv \lim_{k \rightarrow \infty} \rho_\infty^{(k)}. \quad (3.4)$$

Fig. 3 shows the result from the first 100 coefficients; it seems that these expansions converge only for finite values of $x < 2.8$ and $1/|x| < 2.4$ which hints at additional singular points in the complex x -plane. We will locate these *branchpoints* of the W_t -function in Section 5.

At high orders in the above expansions the computational cost of using Lagrange's expansion soon becomes prohibitive. Indeed, the data in Fig. 3 were generated by developing recursion relations for the expansion coefficients in Eqs. (3.1, 3.2). By differentiating Eq. (1.3) with respect to x and eliminating the trigonometric functions one arrives at the simple differential equation

$$W_t'(x) = \frac{W_t(x)}{x + x^2 + W_t^2(x)}. \quad (3.5)$$

Turning first to the expansion around $|x| \rightarrow \infty$, we set $t = 1/x$ and rewrite the above differential equation as

$$(1+t) \frac{d}{dt} \left(\frac{1}{W_t(1/t)} \right) - t^2 \frac{dW_t(1/t)}{dt} = \frac{1}{W_t(1/t)}. \quad (3.6)$$

⁵See, e.g., Ref. [1], Eq. 3.6.5 .

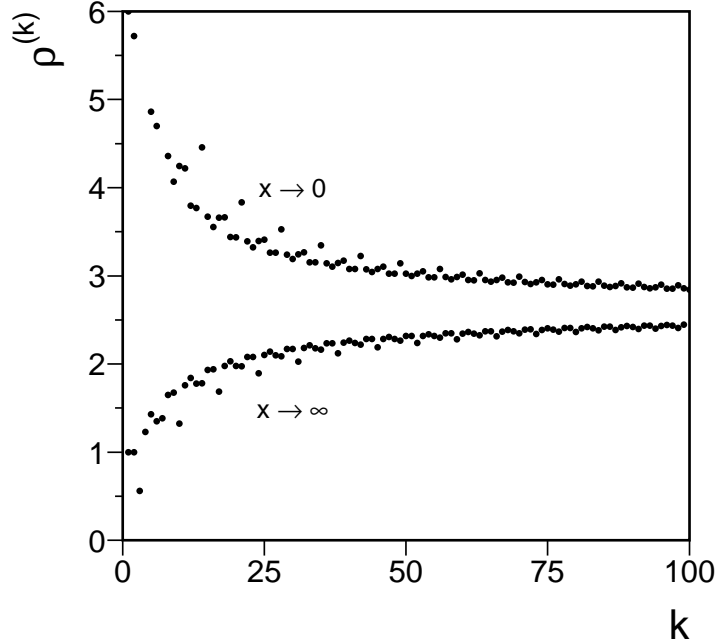


Figure 3: Estimates of the convergence radius for the series expansions (3.1, 3.2) of $W_t^{(1)}(x)$ from the first 100 coefficients.

With the ansatz

$$\frac{1}{W_t(1/t)} = \frac{2}{\pi} \sum_{k=0}^{\infty} c_k t^k \quad (3.7)$$

one obtains a system of coupled recursion relations for the expansion coefficients b_k, c_k

$$(k+1)c_{k+1} + (k-1)c_k = \frac{\pi^2}{4} (1 - \delta_{k0}) (k-1)b_{k-1} \quad (3.8)$$

$$\sum_{j=0}^k b_{k-j} c_j = \delta_{k0}, \quad (3.9)$$

which can be solved successively for $k = 0, 1, \dots$ starting with $b_0 = 1$. For asymptotically large values of k , we find (numerically) that the coefficients b_k approach the simple functional form

$$b_k \xrightarrow{k \rightarrow \infty} \frac{c}{k^{3/2}} (\rho_\infty)^k \sin(ak + b), \quad (3.10)$$

with $c \simeq 0.584$, $a \simeq 2.25$, $b \simeq -3.59$ and the radius of convergence of the expansion in t is $1/\rho_\infty \simeq 1/2.64$ ⁶. Indeed, by writing the trigonometric function as a sum of two

⁶In the quantum electrodynamical context where the W_t -function appeared [8], this implies a *finite* convergence radius of the perturbative expansion contrary to the usual semi-heuristic arguments [9] for an essential singularity at zero coupling constant.

exponentials we find that we can absorb the rapid oscillations in b_k into the definition of a new variable x' (or, equivalently, t'), obtained by rotating x to xe^{ia} (or xe^{-ia} for the second of the two exponentials). Hence we anticipate that the branchpoints responsible for the finite radius of convergence of W_t are in fact located at $x = \rho_\infty e^{\pm ia} \simeq 2.64 e^{\pm 0.72\pi i}$, i.e. in the second and third quadrants of the complex x plane. Furthermore note that, generically, the expansion coefficients of the root $(1 - t\rho_\infty)^\kappa$ behave, at large orders k , like $(\rho_\infty)^k / k^{\kappa+1}$, which leads us to suspect that the branch cuts are of square root type. These suspicions will be confirmed in Section 5.

For $x \rightarrow +0$ on the other hand we set $W_t^{(1)}(x) = \sqrt{x} f(x)$ and obtain the differential equation

$$(x-1)f(x) + 2x(x+1)f'(x) + f^3(x) + \frac{2}{3}x \frac{d}{dx}(f^3(x)) = 0. \quad (3.11)$$

The ansatz

$$f^3(x) = \sum_{k=0}^{\infty} d_k x^k \quad (3.12)$$

now leads to the following system of recursion relations for the coefficients

$$a_k + (1 - \delta_{k0}) a_{k-1} + \frac{1}{3} \frac{2k+3}{2k-1} d_k = 0 \quad (3.13)$$

$$\frac{1}{k} \sum_{j=1}^k (4j-k) a_j d_{k-j} = d_k, \quad k = 1, 2, \dots \quad (3.14)$$

where $a_0 = d_0 = 1$ is the starting point. Eq. (3.14) follows from the identity $f \cdot (f^3)' = 3f^3 \cdot f'$. For large k the recurrence relations yield

$$a_k \xrightarrow{k \rightarrow \infty} \frac{c}{k^{3/2}} (\rho_0)^{-k} \sin(ak + b), \quad (3.15)$$

with $c \simeq 0.564$, $b \simeq -3.14$, $\rho_0 = \rho_\infty$ and a the same as above.

Finally, we note that many integrals over the W_t -function may be performed analytically by a partial integration and changing variables to $x = y \tan y$:

$$\int dx f[W_t(x)] = x f[W_t(x)] - \int dy y \tan y f'(y) \quad (3.16)$$

For example,

$$\int dx \ln[W_t(x)] = x \ln[W_t(x)] + \ln \left| \cos(W_t(x)) \right| \quad (3.17)$$

$$\int dx \ln[\sin(W_t(x))] = x \ln[\sin(W_t(x))] - \frac{1}{2} W_t^2(x), \quad (3.18)$$

and so on.

From the latter equation and the asymptotic behaviour of the W_t -function one immediately obtains the definite integral

$$\int_0^\infty dx \ln[\sin(W_t^{(1)}(x))] = -\frac{\pi^2}{8}. \quad (3.19)$$

In addition one finds

$$\int_0^{\pi/4} dx W_t^{(1)}(x) = \frac{\pi^2}{16} + \frac{\pi}{8} \ln 2 - \frac{1}{2}G \quad (3.20)$$

where $G = 0.91596594\dots$ is Catalan's constant. This is just the special case when Young's inequality (Ref. [2], Eq. 12.315) applied to the integral

$$\int_0^a dx W_t^{(1)}(x) \geq a \frac{\pi}{4} + \frac{\pi}{8} \ln 2 - \frac{1}{2}G, \quad a \leq \frac{\pi}{4} \quad (3.21)$$

becomes an equality due to the relation (2.20).

4 Numerical evaluation and approximations to the $W_t(x)$ -function

4.1 Chebyshev approximation

The numerical evaluation of the W_t -function for real arguments is most easily accomplished by expanding in Chebyshev polynomials [10]

$$W_t^{(1)}(x) = \begin{cases} \sqrt{x} \sum_{k=0} \alpha_k T_k \left(\frac{2x}{a} - 1 \right) & , \quad 0 \leq x \leq a \\ \frac{\pi}{2} \sum_{k=0} \beta_k T_k \left(\frac{a}{x} \right) & , \quad |x| > a \\ \pi \sum_{k=0} \gamma_k T_k \left(\frac{2x}{a} + 1 \right) & , \quad -a \leq x < 0 . \end{cases} \quad (4.1)$$

Table 1 gives the corresponding coefficients for $a = 3.5$, which was found to be a convenient value to use in order to divide the different regions. One should keep in mind that $|T_n(x)| \leq 1$ for $x \in [-1, +1]$, so that (assuming a rapid decrease of the coefficients) the absolute value of the last coefficient gives an estimate of the accuracy with which $W_t^{(1)}(x)$ has been approximated by the truncated Chebyshev expansion.

4.2 Approximation via iteration

To calculate the W_t -function for arbitrary (complex) x , one may naturally try to solve Eq. (1.3) by iteration. In this respect we have found Halley's improvement [11] to the Newton-Raphson algorithm to be useful. After i iterations, this leads to the estimate for the root y of a function $f(y)$ as

$$y_{i+1} = y_i - f(y_i) \left[f'(y_i) - \frac{f(y_i) f''(y_i)}{2f'(y_i)} \right]^{-1}, \quad (4.2)$$

k	α_k	β_k	γ_k
0	0.80600536	1.03465858	0.82312766
1	-0.16766125	-0.28291110	0.16771494
2	0.02302848	0.03258714	0.01423939
3	-0.00298934	0.00177957	-0.00442520
4	0.00030980	-0.00206359	-0.00095545
5	-0.00001275	0.00044900	0.00024196
6	-0.00000478	0.00002021	0.00007926
7	0.00000178	-0.00004188	-0.00001706
8	-0.00000038	0.00001127	-0.00000743
9	0.00000006	0.00000018	0.00000136
10	-0.00000001	-0.00000111	0.00000075
11	0.00000000	0.00000035	-0.00000012
12	0.00000000	-0.00000001	-0.00000008
13	0.00000000	-0.00000003	0.00000001
14	0.00000000	0.00000001	0.00000001

Table 1: Chebyshev expansion coefficients of $W_t^{(1)}(x)$ in Eq. (4.1) for $a = 3.5$.

which, with $f(y) = x - y \tan y$ and x fixed, yields

$$y_{i+1} = y_i + (x - y_i \tan y_i) \left[y_i(1 + \tan^2 y_i) + \tan y_i + \frac{(y_i \tan y_i + 1)(\tan^2 y_i + 1)}{y_i(1 + \tan^2 y_i) + \tan y_i} (x - y_i \tan y_i) \right]^{-1}. \quad (4.3)$$

4.3 A variational principle for $W_t(x)$

The quantum mechanical model of Section 2 can be used to obtain some insight and some approximations for the W_t -function. It is slightly nonstandard because of the energy-dependence of the additional interaction but this energy-dependence is linear so that it

can be easily handled. The Schrödinger equation may be cast into the form

$$H_0 \psi(\xi) = EN(\xi) \psi(\xi) \quad (4.4)$$

with $H_0 = -\hbar^2 d^2/(2m d\xi^2)$ and $N(\xi) = 1 + \lambda \delta(\xi - a/2)$. For a positive definite operator N we can define

$$H = N^{-1/2} H_0 N^{-1/2} \quad , \quad \phi = N^{1/2} \psi \quad (4.5)$$

and end up again with a normal Schrödinger equation $H\phi = E\phi$ for which all standard methods of quantum mechanics can be applied. In view of the finite convergence radius of the series expansion the variational method is of particular interest here as it is a non-perturbative method. It gives an upper bound for the true energy

$$E = \frac{\hbar^2 k^2}{2m} \leq \frac{\langle \phi_t | H | \phi_t \rangle}{\langle \phi_t | \phi_t \rangle} \quad , \quad (4.6)$$

where ϕ_t is a trial state containing variational parameters. Using Eq. (4.5) this can be cast into the form

$$E \leq \frac{\langle \psi_t | H_0 | \psi_t \rangle}{\langle \psi_t | N | \psi_t \rangle} \quad , \quad (4.7)$$

which is a well-known variational principle for the generalized eigenvalue problem (4.4) [12]. Recalling Eq. (2.8) and setting $a = \pi$ for convenience we obtain

$$W_t^2(x) \leq \frac{\pi^2}{4} \int_0^\pi d\xi \left(\frac{d\psi_t(\xi)}{d\xi} \right)^2 \cdot \left[\int_0^\pi d\xi \psi_t^2(\xi) + \frac{\pi}{x} \psi_t^2\left(\frac{\pi}{2}\right) \right]^{-1} \quad , \quad \psi_t(0) = \psi_t(\pi) = 0. \quad (4.8)$$

As usual this variational principle can be applied most easily to the ground state, i.e. to the principle branch. Indeed, taking as trial wave function just the unperturbed ground state wave function $\psi_t(\xi) = \sin \xi$ gives

$$W_t^{(1)}(x) \leq \frac{\pi}{2} \sqrt{\frac{x}{x+2}} \quad , \quad \left(\frac{1}{x} > -\frac{1}{2} \right) \quad (4.9)$$

which covers both limiting cases of the series expansion studied in the previous Section ⁷. However, it predicts a square-root type branchpoint on the real axis at $x = -2$ (where $\langle \psi_t | N | \psi_t \rangle$ vanishes) which obviously is not realistic. One can easily do better by allowing for an admixture of the first excited symmetric state, i.e. $\psi_t(\xi) = \sin \xi + b \sin 3\xi$, where b may be optimized for each value of x . A simple calculation in which we fix the square root sign by demanding that $b \rightarrow 0$ for $x \rightarrow \pm\infty$ then gives

$$W_t^{(1)}(x) \leq \frac{3\pi}{2} \left(\frac{x}{5x + 10 + 2 \operatorname{sgn}(x) \sqrt{25 + 16x + 4x^2}} \right)^{1/2} \quad . \quad (4.10)$$

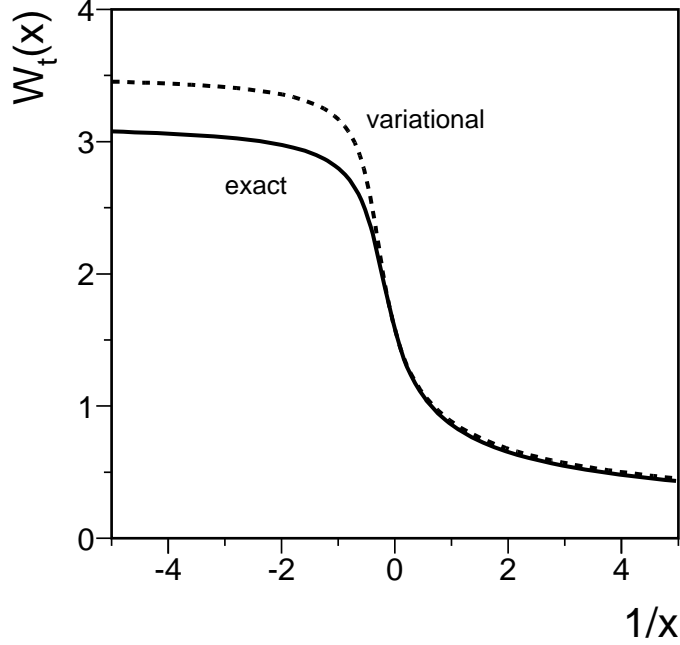


Figure 4: The principal branch of the W_t -function as function of $1/x$, as well as its variational approximation of Eq. (4.10).

This improves the bound near $x = +0$ to $W_t^{(1)}(x) \leq 3\pi\sqrt{5x}/20 = 1.0537\sqrt{x}$ and predicts $W_t^{(1)}(-0) \leq \pi\sqrt{5}/2 = 1.1180\pi$.

Fig. 4 compares this variational approximation with the exact $W_t^{(1)}$ -function calculated numerically via the iteration procedure. For $x > 0$ the agreement is excellent. While the approximation is regular on the negative x -axis it exhibits branchpoints at $x = -2 \pm 3i/2$ in the complex x -plane where the inner square root vanishes. This would restrict the series expansions of $W_t^{(1)}(x)$ around $x = 0$ or $x = \infty$ to converge for magnitudes smaller or larger than $5/2$, respectively. In the next Section we will find that the exact convergence radius is 2.6397 .

⁷Note that $\pi/(2\sqrt{2}) = 1.1107$ so that the bound is also fulfilled near $x = 0$.

5 Analytic structure in the complex plane

5.1 The branch points

The implicit equation (1.3) can be written in the form

$$y = \operatorname{Arctan} \frac{x}{y} = \frac{1}{2i} \operatorname{Ln} \frac{y + ix}{y - ix} \quad (5.1)$$

where Arctan , Ln denote the general (multivalued) inverse tangent and logarithmic functions, respectively. One can immediately see that the function $y = W_t(x)$ is finite in any finite part of the complex x plane. Indeed, the only singularities of the expression on the r.h.s. of Eq. (5.1), as a function of x and y , are the logarithmic branch points at $y = \pm ix$. The latter cannot be satisfied simultaneously with Eq. (5.1) at any finite x . The derivatives of $y = W_t(x)$ have a rather simple structure (in implicit form):

$$y' = \frac{dy}{dx} = \frac{y}{y^2 + x^2 + x} = \frac{\cos^2 y}{y + \sin y \cos y} \quad (5.2)$$

$$y'' = \frac{d^2 y}{dx^2} = -\frac{2xy}{(y^2 + x^2 + x)^2} - \frac{2y^3}{(y^2 + x^2 + x)^3} \quad (5.3)$$

$$y^{(n)} = \frac{d^n y}{dx^n} = \frac{P_n(x, y)}{(y^2 + x^2 + x)^{2n-1}} \quad (5.4)$$

where $P_n(x, y)$ is some polynomial in x and y . The first derivative diverges at the points where

$$y^2 + x^2 + x = 0 \quad (5.5)$$

together with the all higher derivatives. Because all the derivatives have the same polynomial $(y^2 + x^2 + x)$ to an appropriate power in the denominator, they are either all finite or all divergent at the same point x . Therefore, in order to find all singularities of $W_t(x)$ it is sufficient to solve Eq. (5.5); this is equivalent to

$$\sin y \cos y + y = 0 \quad (5.6)$$

which involves only the function value y . One obvious solution is $y_0 = 0$; all other solutions of (5.6) are complex. Setting $2y = u + iv$, where u and v are real, gives

$$u + \sin u \cosh v = 0 \quad (5.7)$$

$$v + \cos u \sinh v = 0. \quad (5.8)$$

We can restrict ourselves to $u > 0$ (if y is a solution of (5.6) then $-y$ is also a solution). Because $\cosh v$ and $\sinh v/v$ are always positive, we get the following constraints from Eqs. (5.7, 5.8)

$$\sin u \leq 0, \quad \cos u \leq 0, \quad (5.9)$$

which leads to

$$(2n - 1) \pi \leq u \leq \left(2n - \frac{1}{2}\right) \pi, \quad n = 1, 2, \dots \quad (5.10)$$

From Eqs. (5.7, 5.8) one gets an equation containing only the variable u :

$$\tan u \cdot \operatorname{arccosh} \left(-\frac{u}{\sin u} \right) = \sqrt{u^2 - \sin^2 u} \quad (5.11)$$

which has exactly one solution u_n in each interval n defined by Eq. (5.10). For large n one finds $u_n = b_n - \ln(2b_n)/b_n + \dots$ where $b_n = (2n - 1/2) \pi$ and therefore

$$\pm y_n = \frac{1}{2} b_n \pm \frac{i}{2} \ln(2b_n) + \mathcal{O} \left(\frac{\ln n}{n} \right) \quad (5.12)$$

$$x_n = -\frac{1}{2} \ln(2b_n) - \frac{1}{2} \pm \frac{i}{2} b_n + \mathcal{O} \left(\frac{\ln n}{n} \right) \quad (5.13)$$

which is in good agreement with the numbers in Table 2 obtained from the numerical solution of Eq. (5.11).

n	x_n	$ x_n $	$\pm y_n$
1	$-1.650611 \pm 2.059981 i$	2.639705	$2.106196 \pm 1.125364 i$
2	$-2.057845 \pm 5.334708 i$	5.717853	$5.356269 \pm 1.551574 i$
3	$-2.278470 \pm 8.522637 i$	8.821948	$8.536682 \pm 1.775544 i$
4	$-2.431122 \pm 11.68877 i$	11.938917	$11.69918 \pm 1.929404 i$
5	$-2.547991 \pm 14.84580 i$	15.062869	$14.85406 \pm 2.046852 i$
6	$-2.642706 \pm 17.99809 i$	18.191069	$18.00493 \pm 2.141891 i$
...			

Table 2: The branch points x_n of $y = W_t(x)$ and the corresponding function values y_n .

To investigate the type of the singularities we introduce new variables Δx and Δy in the vicinity of the singular point x_n :

$$x = x_n + \Delta x, \quad y = y_n + \Delta y. \quad (5.14)$$

The implicit equation (1.3) can now be rewritten in the form

$$\Delta x \cos(y_n + \Delta y) = (\Delta y \cos \Delta y - \sin \Delta y) \sin y_n + \Delta y \sin \Delta y \cos y_n. \quad (5.15)$$

If we go along a closed contour around the point y_n in the complex y plane assuming that Δy is sufficiently small, then the corresponding path in the complex x plane will make a closed contour winding up twice as many times around the corresponding point x_n . This can be demonstrated by inspecting the leading term in the expansion of Eq. (5.15) in powers of Δy :

$$\Delta x \cos y_n = (\Delta y)^2 \cos y_n + \mathcal{O}((\Delta y)^3) \quad (5.16)$$

Therefore all singularities of $W_t(x)$ are of square root type : $\Delta y = \pm(\Delta x)^{1/2} + \dots$ or

$$W_t(x) \xrightarrow{x \rightarrow x_n} W_t(x_n) \pm \sqrt{x - x_n}. \quad (5.17)$$

Another way to obtain this result is to insert the following ansatz

$$W_t(x) \xrightarrow{x \rightarrow x_n} W_t(x_n) + c (x - x_n)^\kappa \quad (5.18)$$

into the differential equation (3.5). Here κ must be positive since we know that $W_t(x_n)$ exists. Assuming $\kappa < 1$ we obtain in leading order

$$\kappa c (x - x_n)^{\kappa-1} = \frac{1}{2c} (x - x_n)^{-\kappa} \quad (5.19)$$

which determines $\kappa = 1/2$ and $c^2 = 1$.

5.2 The Riemann surface

Since the function $W_t(x)$ has an infinite (countable) number of branch points, it has an infinite number of Riemann sheets as was already clear from Fig. 2. Therefore the question arises how to define these Riemann sheets in the most convenient way for any particular purpose. As we know the position and the type of all branch points, it only remains to define the cuts originating from these branch points. Given the cuts (we call any complete set of them a *scheme*), one then only needs to know how the different Riemann sheets are connected across the cuts.

It turns out that the labeling of the Riemann sheets based on the inspection of the function on the real x -axis without a proper consideration of the branch points, as was done in Section 2, is not very illuminating when the whole complex x -plane is concerned. Below we consider two other schemes of Riemann sheets which are better suited for the discussion of the singularities and analytical continuation across the cuts. In order to keep notations simple we prefer not to indicate the particular scheme explicitly in the notation $W_t^{(n)}(x)$; it will be defined in the context whenever the scheme is relevant.

The first new scheme of Riemann sheets is demonstrated in Fig. 5 where the cuts originating from the branch points x_n run to $-\infty$ along the lines of constant imaginary

sheet	...	-1	1	2	3	...	n	...
$\lim_{x \rightarrow +\infty} W_t^{(n)}(x)$...	$-\pi/2$	$\pi/2$	$3\pi/2$	$5\pi/2$...	$\text{sgn}(n)(n - 1/2)\pi$...
$\lim_{x \rightarrow +0} W_t^{(n)}(x)$...	-0	+0	π	2π	...	$\pi(n - 1)$...

Table 3: The scheme of Riemann sheets where the cuts extend to $-\infty$ as shown in Fig. 5.

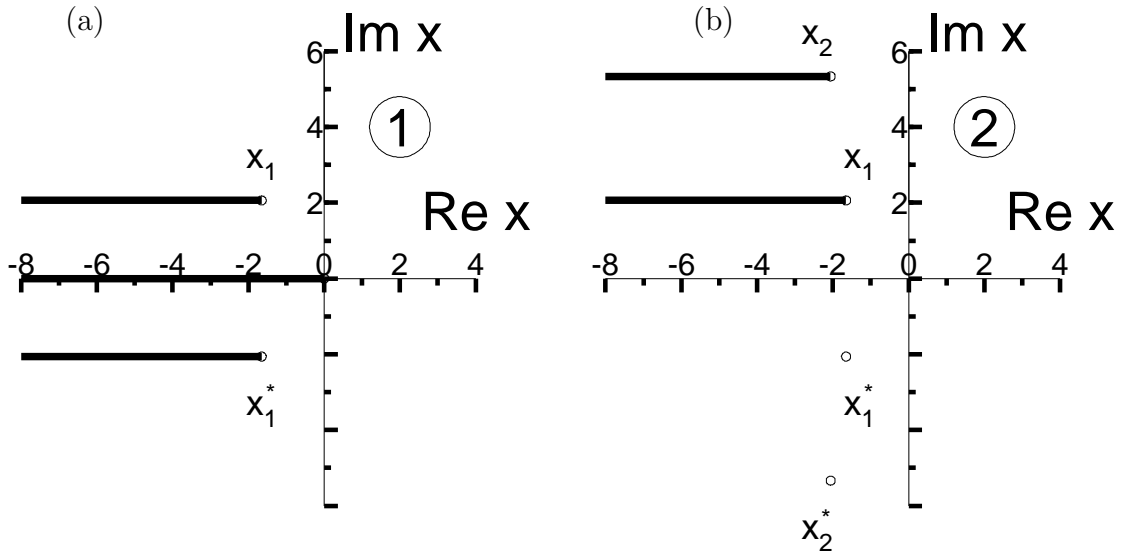


Figure 5: The Riemann sheets of $y = W_t(x)$ in the scheme where all cuts go to $-\infty$: (a) sheet 1, (b) sheet 2.

part $\text{Im } x = \text{Im } x_n$, $-\infty < \text{Re } x \leq \text{Re } x_n$. Every Riemann sheet can be uniquely specified by the limit values at $x \rightarrow +\infty$ or $x \rightarrow +0$ as given in Table 3.

There is a finite number of cuts on every sheet. The connection between different sheets is demonstrated in Fig. 5. On all sheets n except $n = \pm 1$, the function $W_t(x)$ is continuous and real on the real x axis. On the sheets $n = \pm 1$, the function is real for $x \geq 0$ and purely imaginary for $x < 0$.

Sending all cuts to infinity has, however, a drawback: it obscures the analytical properties of $W_t(x)$ at $x = \infty$. In fact, the points $x = \infty$ correspond to the regular points $t = 1/x = 0$ of the function $W_t(1/t)$. In the case when the analytical properties at infinity

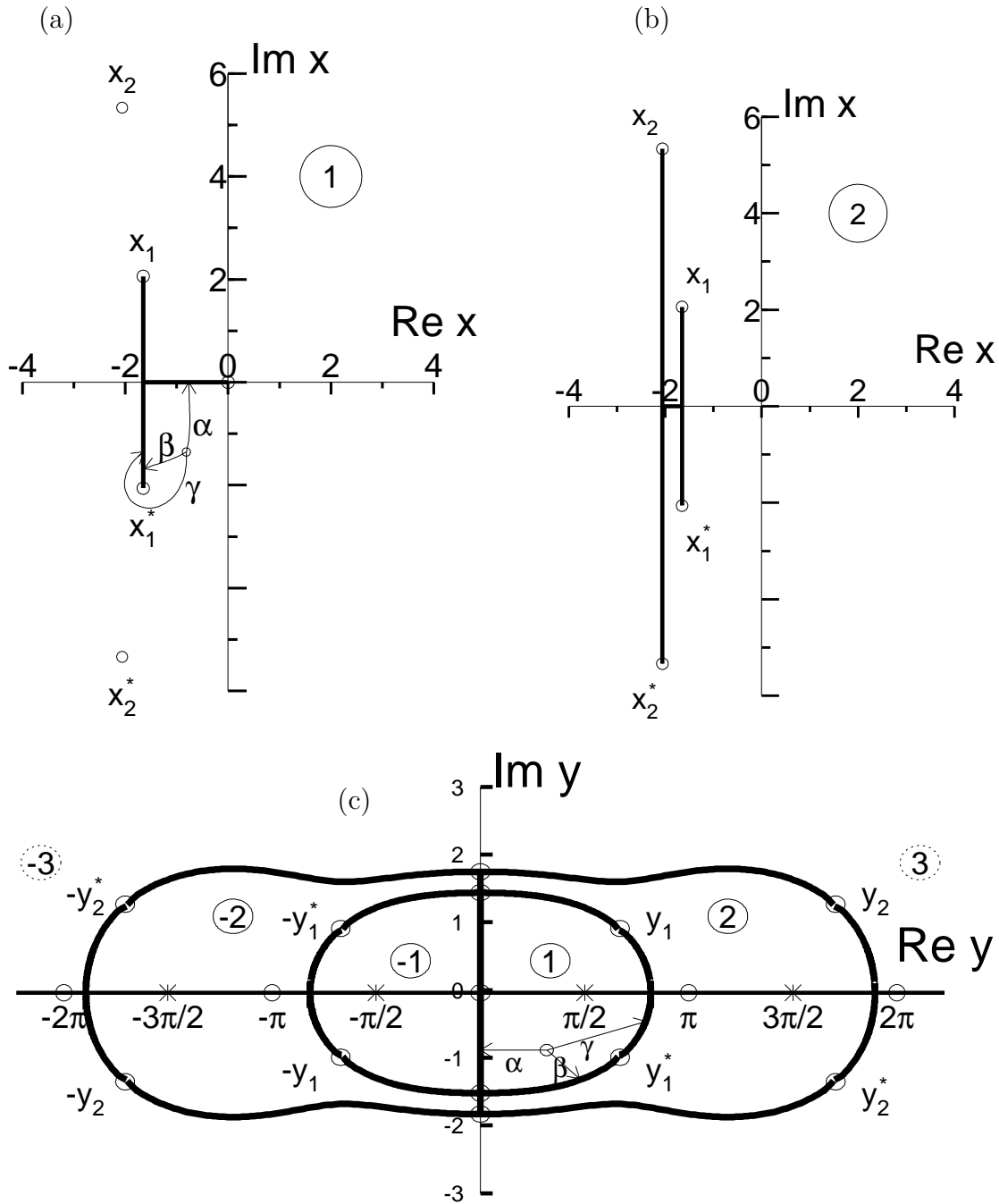


Figure 6: The Riemann surface of $y = W_t(x)$: (a) sheet 1, (b) sheet 2, and (c) the images of different sheets in the complex y plane. The path α in plot (a) goes from sheet 1 to sheet -1 across the cut $(\text{Re } x_1, 0)$, the corresponding image of this path in the y plane is shown in plot (c). The paths β and γ go from sheet 1 to sheet 2 across the cuts $(\text{Re } x_1, x_1^*)$ and (x_1, x_1^*) respectively.

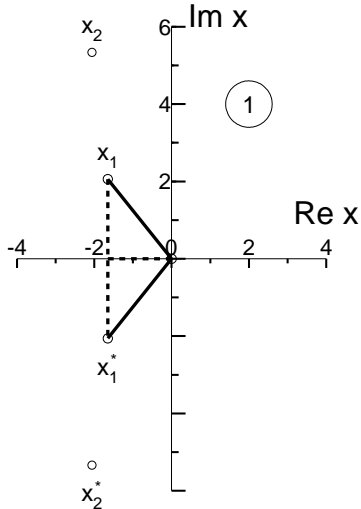


Figure 7: A modification of the main Riemann sheet of $y = W_t(x)$ shown in Fig.6 (a): the cut between x_1 and x_1^* is deformed so that it crosses the real x -axis by going over the branch point $x = 0$.

are of interest, alternative schemes of the Riemann surface, such as shown in Fig. 6, have definite advantages. This second new scheme provides a convention of branches which is very suitable for the quantum mechanical example in Section 2, where the argument x was proportional to the inverse coupling constant so that the perturbative expansion became an expansion of W_t around $x = \infty$. In this scheme all cuts are finite in the complex x -plane: every branch point x_n ($n = 1, 2, \dots$) is connected with the corresponding complex conjugated point x_n^* , and every sheet, except for the sheets ± 1 , has a pair of such cuts. By deforming the cut connecting the branch points x_1 and x_1^* as shown in Fig. 7 one can make it cross the real x -axis at $x = 0-$, so that the function is made continuous at both $x > 0$ and $x < 0$, as in the case considered in Section 2. However, this comes at the price of having the branch point at $x = 0$ superimposed on the cut between x_1 and x_1^* , which is not very convenient for the purpose of analytical continuation.

The cut originating at $x_0 = 0$ occurs on every sheet in a finite interval: on the sheets ± 1 it goes along the real axis from zero to the cut connecting x_1 and x_1^* , on all other sheets it lies on the real axis between the two cuts connecting x_n with x_n^* and x_{n-1} with x_{n-1}^* . For every sheet n all the cuts are located within the limits $|x| \leq |x_n|$, $\text{Re } x_n \leq \text{Re } x \leq \text{Re } x_{n-1}$. The Riemann sheets in this scheme can be uniquely specified by the function values at infinity, which is a regular point on every sheet (see Table 4).

This scheme will be used below in all references to different branches of $W_t^{(n)}(x)$. The

sheet	...	-1	1	2	3	...	n	...
$\lim_{x \rightarrow \infty} W_t^{(n)}(x)$...	$-\pi/2$	$\pi/2$	$3\pi/2$	$5\pi/2$...	$\text{sgn}(n)(n - 1/2)\pi$...

Table 4: The scheme of Riemann sheets with the finite cuts shown in Fig. 6.

sheets n and $-n$ differ only by the function sign: if $y = W_t^{(n)}(x)$, then $-y = W_t^{(-n)}(x)$ (see Eq. (2.19)). The connection between different sheets is shown in Fig. 6.

The simplest way to investigate this connection is to begin with some path in the y plane (image) that connects two points on different sheets for the same x and to calculate the corresponding path in the x plane using Eq. (1.3). For any $n = \pm 1, \pm 2, \dots$, the sheets n and $-n$ are connected to each other across the cut on the real axis between the points $\text{Re } x_n$ and $\text{Re } x_{-n}$ (see the path α in Figs. 6 (a,c)). The cut between the branch points x_n and x_n^* connects the sheet n with the sheet $(n+1)$ for $n > 0$ or with the sheet $(n-1)$ for $n < 0$ (the paths β and γ in Figs. 6 (a,c)). The structure of the cuts for all sheets with $|n| > 2$ is similar to that of sheet 2 (see Fig. 6 (b)).

The definition of $W_t(x)$ as an implicit function, Eq. (1.3), involves the function $y \tan y$ which is *single valued* on the compactified complex plane. Therefore for any y there is *one and only one* value of x such that $W_t(x) = y$. This allows us to determine the topology of any part of the Riemann surface by inspecting its projection onto the y plane. The topological structure of the Riemann surface of $W_t(x)$ turns out to be quite simple: any set of connected Riemann sheets with $n = \pm 1, \pm 2, \dots, \pm n_{max}$ is homeomorphic to a two-dimensional disk as illustrated in Fig. 6 (c). For example, the part of the Riemann surface that consists of four sheets with $n = \pm 1, \pm 2$ is a manifold with a boundary homeomorphic to the one-dimensional sphere S^1 . The Euler characteristic ⁸ of this manifold is $\chi = 1$. This is equal to the Euler characteristic of a disk with a boundary. If this manifold is extended by adding pairs of sheets connected to its boundary ($n = \pm 3, \pm 4, \dots$) then the Euler characteristic remains unchanged. While much more could be said about the topological structure of the Riemann surface a further discussion is beyond the scope of this paper. We close by pointing out that, in a certain sense, the Riemann surface of $W_t(x)$ resembles an elaborate *origami* where a square of paper (which is topologically

⁸This is the topological invariant given by $\chi = V - L + S$ where L , V , and S are the number of vertices, links and faces respectively in a triangulation of the manifold (see e.g. Ref. [13]). For example, the triangulation with the vertices corresponding to the branch points and the links corresponding to the cuts in Figs. 6 (a,b) has $V = 13$, $L = 16$, $S = 4$.

equivalent to a two-dimensional disk) is folded⁹ into a beautiful shape *without paper cuts*. The same property holds true for every function defined by an implicit equation involving any functions that are single-valued at finite x .

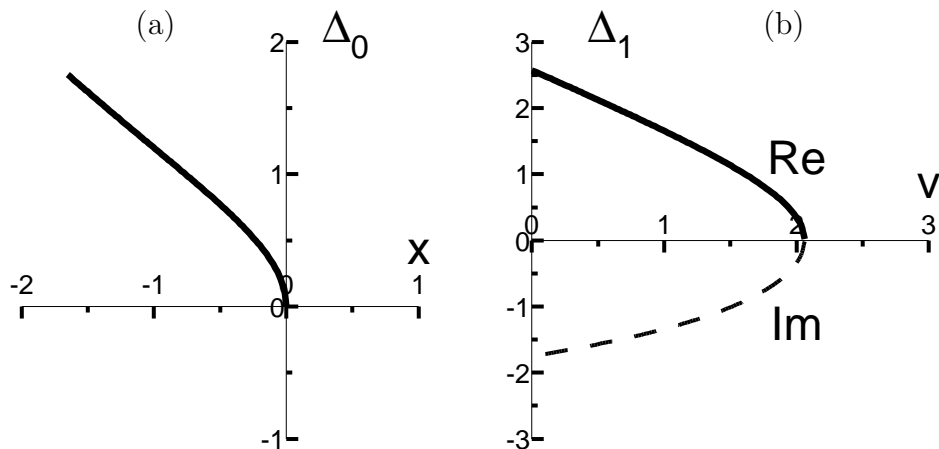


Figure 8: (a) The imaginary part of the discontinuity of $W_t^{(1)}(x)$ across the cut $-\infty < x \leq 0$, (b) the discontinuity of $W_t^{(1)}(x)$ across the cut connecting x_1 and x_1^* .

5.3 The dispersion relation for $W_t(x)$

The analytic structure discussed above allows to derive the dispersion relation satisfied by $W_t(x)$ on the first sheet

$$W_t^{(1)}(z) = \frac{\pi}{2} + \frac{1}{\pi} \int_a^0 du \frac{\Delta_0(u)}{u-z} + \frac{1}{\pi} \int_0^b dv \left(\frac{\Delta_1(v)}{a+iv-z} + \frac{\Delta_1^*(v)}{a-iv-z} \right), \quad (5.20)$$

$$a = \operatorname{Re} x_1, \quad b = \operatorname{Im} x_1. \quad (5.21)$$

Here $\Delta_0(u)$ and $\Delta_1(v)$ are determined by the discontinuities across the cuts on sheet 1 (see Fig. 8):

$$\Delta_0(u) = \frac{1}{2i} [W_t^{(1)}(u+i\epsilon) - W_t^{(1)}(u-i\epsilon)] = \operatorname{Im} W_t^{(1)}(u+i\epsilon), \quad -\infty < u \leq 0 \quad (5.22)$$

$$\Delta_1(v) = \frac{1}{2} [W_t^{(1)}(a+\epsilon+iv) - W_t^{(1)}(a-\epsilon+iv)] \quad , \quad 0 \leq v \leq b. \quad (5.23)$$

⁹The origami paper is not stretched, so the analogy ceases to be valid when we want to deform the disk into the Riemann surface under consideration.

6 Concluding remarks

In the preceding Sections we have derived a number of results on the analytic structure, the numerical evaluation, series expansions and a simple quantum mechanical problem where the function $W_t(x)$ makes its appearance. While certainly not being exhaustive, these results demonstrate the amazingly rich structure and the fascinating properties of the W_t -function which is defined by a simple, implicit equation. We hope that our selected findings may be useful for other researchers encountering this function. Of course, the methods used may be also adapted to related functions and indeed one might also consider, at the expense of convenience, more general implicit equations of which Eq. (1.3) is just a special case. For example, Wright has elaborated [14] on equations of the form

$$(z + b) e^{z+a} = z - b \tag{6.24}$$

and discussed the real solutions z to these equations as a function of a and b in Ref. [15]. Eq. (1.3) may be brought into this form, with $a = 0$ and $b = 2x$, by writing the trigonometric function in its exponential form and setting $W_t = iz/2$. Our results in Section 2 (and elsewhere) would then correspond to purely imaginary, special solutions of Wright's equation.

References

- [1] Abramowitz, M. and Stegun, I. (eds.) : *Handbook of mathematical functions*, (Dover, New York) 1965.
- [2] Gradshteyn, I. S. and Ryzhik, I. M. : *Table of integrals, series and products*, 4th edition, (Academic Press, New York) 1980.
- [3] Goldstein, H. : *Classical Mechanics*, 2nd edition, (Addison-Wesley, Reading) 1980, p. 101. Note the misprint on page 124 which gives the expansion of the solution in terms of Bessel functions.
- [4] Corless, R. M., Gonnet, G. H., Hare, D. E. G., Jeffrey, D. J. and Knuth, D. E., Adv. Comp. Math. **5** (1996) 329.
- [5] Bellman, R. : *Methods of nonlinear analysis*, vol. 1, p. 213, (Academic Press, New York) 1970.
- [6] Shirkov, D. V., Theor. Math. Phys. **119** (1999) 438; Magradze, B. A., Int. J. Mod. Phys. A **15** (2000) 2715; Maxwell, C. J. and Mirjalili, A., Nucl. Phys. B **577** (2000) 209; Gardi, E., Grunberg, G. and Karliner, M., JHEP **9807**(1998) 007.
- [7] Rosenfelder, R., Ann. Phys. (N. Y.) **128** (1980) 188; erratum: Ann. Phys. (N. Y.) **140** (1982) 203.
- [8] Alexandrou, C., Rosenfelder, R. and Schreiber, A. W., Phys. Rev. D **62** (2000) 085009.
- [9] Dyson, F. J., Phys. Rev. **85** (1952) 631; Itzykson, C., Parisi, G. and Zuber, J.-B., Phys. Rev. D **16** (1977) 996; Le Guillou, J. C. and Zinn-Justin, J. (eds.): *Large-order behaviour of perturbation theory*, (North-Holland, Amsterdam) 1990.
- [10] Press, W. H., Flannery, B. P., Teukovskiy, A. A. and Vetterling, W. T. : *Numerical recipes*, chapter 5.8, (Cambridge University Press, Cambridge) 1994.
- [11] For the original reference to this *Methodus Nova Accurata . . .*, see Halley, E., Phil. Trans. Roy. Soc. London **18** (1694) 136; more recent discussions of this method, including interesting historical remarks may be found in, for example, Bateman, H., Amer. Math. Monthl. **45** (1938) 11 and Traub, J. F., Comm. of the Assoc. for Computing Machinery **4** (1961) 276.
- [12] Morse, M. and Feshbach, H. : *Methods of theoretical physics*, vol. 2, (McGraw Hill, New York) 1953.

- [13] Massey, W. S. : *A basic course in algebraic topology*, Graduate Texts in Mathematics 127, (Springer, New York) 1991.
- [14] Wright, E. M., Bull. Am. Math. Soc. **66** (1960) 277; Proc. Roy. Soc. Edin. A **65** (1960/61) 358.
- [15] Wright, E. M., J. Soc. Indust. Appl. Math. **9** (1961) 136.